Modulation of learning-dependent plasticity in the attention network

Contò[1], F., Ellena[1], G., Edwards[2], G., and Battelli[1,3], L.

[1]Center for Neuroscience and Cognitive Systems@UniTn, Istituto Italiano di Tecnologia, Corso Bettini 31, 38068 Rovereto (TN), Italy

[2]National Institutes of Health, Bethesda, Maryland 20892, USA

[3]Berenson-Allen Center for Noninvasive Brain Stimulation, Department of Neurology, Beth Israel Deaconess Medical Center, Harvard Medical School, Boston, MA 02215

Corresponding Author:

Federica Contò: federica.conto@iit.it

Competing financial interests:

The authors declare no competing financial interests.

Abstract

Neuromodulatory interventions are gaining interest for their potential to enhance key cognitive functions, including attention and learning. However, their effects on cortical activity during training remains limited. Our previous work demonstrated that bilateral transcranial random noise stimulation (tRNS) over the intraparietal sulcus (IPS), coupled with a multi-session attention-based perceptual learning increased functional connectivity within the dorsal-ventral attention network at rest (DVAN, Contò et al., 2021). In this follow-up study we examined how the same multi-session stimulation protocol modulates BOLD signal in the DVAN during two attention tasks. Our findings show that tRNS targeting the IPS selectively enhanced BOLD responses during a spatial, but not a temporal task, indicating task-specific neural effects. Conversely, BOLD responses in the DVAN significantly decreased after sham. Control analyses within the default mode network (DMN) showed no significant changes, indicating the network specific effects of tRNS. The region-specific nature of these effects suggests that tRNS-induced modulation is constrained to key network nodes, enhancing the DVAN's cortical response in spatial tasks, a response that instead decreases after sham and has no benefit on behavior. This selectivity of the cortical response aligns with theories of neural efficiency, indicating that tRNS may prevent natural downregulation in task-relevant areas and promotes sustained plasticity. Our results highlight the potential of tRNS in augmenting cognitive training, providing a powerful tool for the precise modulation of attention networks in both healthy individuals and clinical population.

Introduction

Perceptual learning, the sustained improvement of sensory abilities through visual experience and practice ([1], [2], [3]), is a powerful demonstration of the remarkable adaptability of the human brain. This experience-induced improvement, and the concomitant neural plasticity ([4], [5], [6], [7]), play a fundamental role in our ability to navigate the complexities of the world. PL also provides valuable insights into the adaptive capabilities of the human brain and has practical implications for the design of interventions aimed at improving or restoring sensory perception and cognitive abilities.

PL is intertwined with attentional processes, with the dorsal-ventral cortical attention network ([8], [9], [10]) playing a critical role in orchestrating these cognitive dynamics. When individuals engage in perceptual training, attention typically guides the selection and processing of relevant sensory information ([11], [12], [13], [14], [15], [16], [17], [18]). Consistent with behavioral evidence, fMRI studies have identified the neural substrates involved in this attentional engagement, revealing distinct activation patterns within the dorsal and ventral attentional networks corresponding to different aspects of attention ([7], [11], [19]). The dorsal attention network (DAN), including the intraparietal sulcus (IPS) and the frontal eye fields (FEF), is primarily responsible for goal-directed or top-down attentional control ([20]). This network directs attention to specific spatial locations or features based on cognitive goals and task instructions. In contrast, the ventral attention network (VAN), centered around regions such as the temporoparietal junction (TPJ) and the ventral frontal cortex (VFC), is specialized for detecting behaviorally relevant or salient stimuli, which capture attention even when they are unrelated to current goals ([21]). One hypothesis is that the ventral attention network serves as a bottom-up attention system that automatically highlights stimuli that are potentially important for task performance and, in general, for survival.

The anatomical connectivity of these attention networks has been explored using diffusion magnetic resonance imaging (dMRI) and fiber tracing techniques. These studies have identified the white matter pathways that connect the major areas of the DAN, such as the dorsal superior longitudinal fasciculus ([22], [23]), as well as those that connect the major areas of the VAN, such as the ventral superior longitudinal fasciculus ([24], [25]). These studies also identified the anatomical regions that connect the DAN and VAN, providing a communication pathway between

the two attentional systems ([22]). The two networks are not only anatomically connected, but also exhibit important connections at the functional level. Indeed, the bidirectional interaction between the dorsal and ventral attention networks (DVAN) allows for flexible and adaptive attentional processing. This interaction is critical for integrating top-down and bottom-up signals, thereby enhancing the overall efficiency and responsiveness of the attention system beyond the capabilities of each network operating individually ([21], [26]). While behavioral and imaging studies highlight attention as a critical function in shaping cognitive processes associated with learning, a complete understanding of the interplay between training, plasticity and attention is still lacking.

Recent efforts to improve perceptual training gains have introduced novel interventional methods such as transcranial electrical stimulation (tES; ([27], [28], [29], [30]). tES is a safe non-invasive method of modulating brain activity using two or more electrodes ([31], [32], [33]). Although the mechanism of action of these techniques is not yet fully understood, physiological studies suggest that direct current stimulation can facilitate or inhibit neuronal firing by altering the membrane voltage ([34], [35]). Direct current has also been shown to increase local field potential and affect distal cortical areas ([36]). In addition to modulating cortical excitability, tES has been shown to have beneficial effects on perception and cognition ([28], [37], [38], [39], [40]). Among these approaches, transcranial random noise stimulation (tRNS) is a specific form of tES that delivers alternating current stimulation at random frequencies, which can modulate visual cortex excitability ([41]) and improve performance in perceptual learning tasks ([42], [43], [44], [45]). Several studies have shown that tRNS exerts a neuromodulatory effect that often results in greater neurophysiological and behavioral after-effects compared to other techniques ([46], [47], [48]; for a review on tRNS see [49]). However, the effects of tRNS on brain dynamics and the concurrent behavioral facilitation during learning have been investigated in only few studies ([7], [50]).

This study aims to investigate the impact of tRNS on cortical dynamics when coupled with perceptual learning, focusing specifically on the involvement of the dorsal and ventral attention networks. Our goal is to study the neural substrate of adaptive changes in sensory processing associated with learning. In a previous study, we analyzed resting-state functional data collected during the pre- and post-training sessions of a perceptual learning procedure coupled with tRNS.

We found that tRNS delivered over the attention-related areas of the parietal cortex increased functional connectivity at rest within nodes of the attention network and boosted perceptual

learning ([7]). The strong enhancement of behavioral performance correlated with increased functional connectivity within the main nodes of the DVAN, likely strengthening the interaction between these two subnetworks. These results suggested that concurrent training and stimulation modulate large-scale cortical dynamics, strengthen functionally selective neural pathways after training, and represent a potential physiological marker of lasting changes induced by multi-session tRNS.

While the previous study focused on cortical dynamics during rest, in the present study we analyzed the cortical dynamics within the attention network occurring *during* the active engagement of participants in attention tasks (specifically, a cross-task paradigm involving an orientation and a temporal attention task) and compared these dynamic changes before and after training. While in our previous study we analyzed changes within the attention network during resting-state conditions, we now sought to understand changes in cortical dynamics occurring after active engagement in perceptual learning tasks. We thus analyzed task-related cortical response to investigate the dynamic of BOLD activity within the primary nodes of the DVAN to understand how it is affected by multi-session tRNS combined with cognitive training. We found that task-related hemodynamic cortical response increased after parietal stimulation and cognitive training, resulting in significantly improved performance in perceptual learning, while we found no changes in BOLD response and behavior after stimulation over the active control area hMT or after sham, thus demonstrating the critical role of tRNS in modulating attentional control to refine perceptual skills and promote neural plasticity.

Results

We conducted task-related fMRI analysis to investigate the impact of multi-session tRNS combined with training on long-term modulation of the BOLD signal during two tasks: an orientation discrimination (OD) and a temporal order judgment (TOJ) task. Participants underwent fMRI scanning during both pre- and post-test sessions (S2 and S7, *Figure 4*; *Methods* section), during which they performed the two attentional tasks (details relative to the tasks and stimuli used can be found in the *Methods* section). In the training phase, which took place between the two fMRI sessions, all subjects were asked to perform two tasks simultaneously, alternated every trial, and they were assigned to three different groups. One group received tRNS over the bilateral IPS,

our crucial hotspot for visuospatial attention ([8], [51]) and a central hub for the DVAN ([52]). A second group received tRNS over the bilateral human middle temporal (hMT) areas (active control condition) and a third group received Sham stimulation. Of note, the active control condition was particularly challenging given the close proximity of the hMT to the IPS, but it was important to test both areas as they are part of the DVAN but may contribute differently to visuospatial processing and thus may respond differently to stimulation and training.

To evaluate the impact of multi-session tRNS combined with task training, we measured changes in the BOLD signal between pre- and post-test session for each task individually. Single-subject deconvolution analysis was performed to examine the BOLD responses between the two different stimuli conditions (orientation and temporal stimuli). Peaks of the individual deconvolved beta weights relative to the ROIs embedded in the DVAN were analyzed to evaluate the impact of stimulation combined with training on the attentional network. In addition, to control for network-specific effects of stimulation, we also investigated whether tRNS and training impacted cortical activity within a different (control) network, the default mode network (DMN), which is typically active during passive or resting conditions ([25], [53], [54], [55]). Next, we compared the change in beta weights measured within the DVAN and the DMN to test whether these two networks showed different modulation of the BOLD activity measured within their main ROIs after stimulation. Finally, we investigated the change in beta weights of each single ROI embedded in the attentional network across different conditions. Details of data analysis pipeline can be found in the Methods section.

Impact of stimulation on the DVAN

We first ensured that the three stimulation groups did not differ in brain activity at baseline by comparing their beta weights on the pre-test fMRI session for each task. To do so, we fitted a linear mixed effects model (LMM) to examine the effect of different stimulation conditions on the normalized beta weights measured during the pre-test, while accounting for individual and ROIs differences (the model included random intercepts for subjects and for brain areas). The Type II Wald Chi-Square test for the Stimulation Condition effect factor yielded a Chi-square value of 4.102 ($\chi^2(2) = 4.102$, $p = 0.129$, *lmer*) for the OD task and 1.717 ($\chi^2(2) = 1.717$, $p = .423$, *lmer)* for the TOJ task, indicating that the overall effect of different stimulation conditions on beta weights was not statistically significant at baseline for either task.

Next, delta scores representing the difference between pre- and post-stimulation beta weights were computed at the individual subject level ($\Delta\beta = \beta$(fMRI post-test) – β(fMRI pre-test) and per single ROI to quantify changes in BOLD signal modulation. These ROIs include key areas such as the anterior, posterior, and central intraparietal sulcus (IPS), human middle temporal (hMT), frontal eye fields (FEFs), temporal parietal junction (TPJ), ventral frontal cortex (VFC), and inferior frontal junction (IFJ), covering both dorsal and ventral attention networks (see *Methods* section for a complete list of the ROIs included in the DVAN, and the relative Talairach coordinates). The delta values reflect the changes in in BOLD signal modulation normalized to baseline activity, before stimulation. An LMM was then fitted to examine the combination of stimulation and training on subjects' delta beta weights (normalized delta beta weights were modeled as a function of Stimulation conditions, with random intercepts for subjects and brain areas). This analysis revealed a main effect of stimulation group on delta beta weights in response to the OD task ($\chi^2(2) = 12.787$, $p = .0017$, *lmer)*, indicating that changes in beta weights were significantly modulated by the type of stimulation received during training (*Figure 1*). We then compared delta values between different stimulation conditions, and found a significant difference between the Parietal and Sham group with an estimate of 0.678 (SE=0.193, p=.0041 FDR adjusted), and between the Parietal and hMT group with an estimate of -0.442 (SE=0.189, p=0.039 FDR adjusted), indicating that the Parietal condition resulted in significantly higher delta beta weights compared to the Sham and hMT condition (*Figure 1*). No significant difference was found when comparing delta values of the hMT and Sham condition (estimate of 0.236; SE=.189; *p*=.2207 FDR adjusted), indicating that the difference of delta beta weights was not modulated differently between these two conditions. Further analysis of the estimated marginal means (EMMeans), used to summarize the effects of different factors in the linear model, revealed that the average delta values for the Parietal condition was of 0.335 (SE=0.141, with a 95% CI of 0.049 and 0.621), while for the Sham the average delta beta weights was of -0.343 (SE=0.141, with a 95% CI of -0.63 and -0.057), and for the hMT condition of -0.107 (SE=.135, with a 95% CI of -.383 and .0167). These data suggest that parietal stimulation significantly increased delta beta weights, while the Sham condition significantly decreased them. Whereas, the hMT condition did not have a statistically significant effect on the delta beta weights in the DVAN during the OD task.

We then analyzed the effect of different stimulation conditions on the normalized delta beta weights measured in the ROIs of the DVAN during the temporal task (TOJ) using a similar LMM

as for the OD task (normalized delta beta weights relative to the TOJ task were modeled as a function of Stimulation conditions, with random intercepts for subjects and brain areas). The Type II Wald Chi-Square test revealed no significant effect of stimulation condition on the normalized delta beta weights ($\chi^2(2) = 1.917$, $p = .3834$, *lmer*), indicating that the type of stimulation condition did not significantly influence the changes in beta weights for the TOJ task. Pairwise comparison run following the model between conditions showed indeed no significant differences between any pair of conditions (hMT vs Parietal comparison estimate of -0.274, SE=.198, p=.361 FDR-adjusted; Parietal vs Sham comparison estimate of 0.14, SE=.202, p=.768 FDR-adjusted; hMT vs Sham comparison estimate of -0.134, SE=0.198, p=.779 FDR-adjusted). This result is not surprising, as we also found no stimulation or behavioral effect in the TOJ task in our previous study ([7]).

Next, to control for network-specific effects of stimulation, we also analyzed changes in BOLD activity within the DMN, which we hypothesized would not to be affected by the stimulation protocol nor by the training phase. We conducted the same analysis as for the DVAN nodes. Therefore, we first fitted an LMM to examine whether there was a difference in beta weights at baseline (with random factors being subjects and brain areas). No significant main effect was found for the OD task ($\chi^2(2) = 0.967$, $p = .616$, *lmer*), nor for the TOJ task ($\chi^2(2) = 0.357$, $p = .836$, *lmer)*, indicating that beta weights measured at baseline did not differ between the three stimulation groups in this control network. Next, as for the DVAN, delta scores were also calculated for each ROI of the DMN to quantify changes in BOLD signal modulation ($\Delta\beta = \beta$(fMRI post-test) – β(fMRI pre-test) and were used to fit an LMM that examined the effect of stimulation and training on delta beta weights changes (with random intercepts for subjects and ROIs). No main effect of stimulation condition was found on delta beta weights in response to either the OD task ($\chi^2(2) = 1.446$, $p = .4851$, *lmer)*, nor the TOJ task ($\chi^2(2) = 0.565$, $p = .7538$, *lmer),* indicating that beta weights changes were not differently modulated by the type of stimulation received during training (*Figure 1*). Hence, no significant changes were found in any analysis run for the DMN.

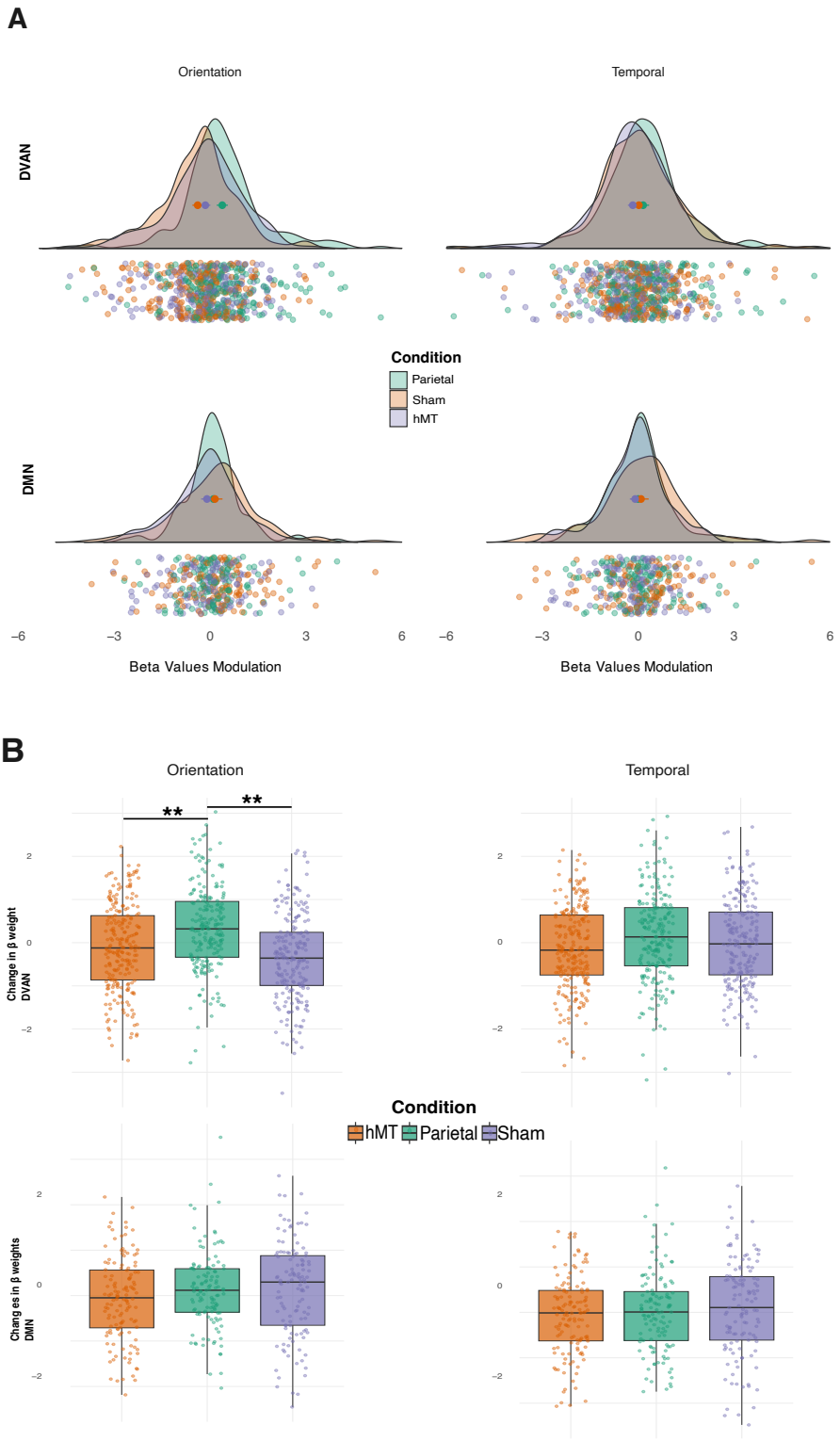

Figure 1. Modulation of Beta weights across different stimulation conditions and networks in response to the two attention tasks (OD and TOJ). A. *Change of Beta weights frequency*

distribution for each stimulation condition computed as the difference between beta weights pre- and post-test session ($\Delta\beta$ = β*(fMRI post-test)*− β*(fMRI pre-test)); orange for hMT, green for Parietal and violet for Sham). Single bold Dots within distributions indicated the median for each stimulation condition, while dots below the distribution curves represents individual data measured for each participant in each of the ROIs embedded in the two networks (Top panel: DVAN, bottom panel: DMN) in response to each type of task stimuli (Orientation on the left and Temporal on the right).* ***B.*** *Box plots for* β*-weights changes by stimulation condition in response to the OD (left Panel) and the TOJ task (right Panel) normalized to baseline, prior to stimulation. The center line in the middle of the box is the median of each data distribution, while the box represents the interquartile range (IQR), with the lower quartile representing the 25th percentile (Q1) and the upper quartile representing the 75th percentile (Q3). Dots represents individual subjects' data. Lines beyond the box represent the minimum and maximum values in the data. Asterisks indicate significant differences between two stimulation condition.*

Finally, to investigate the specificity of the effect of tRNS during training on attention task, we further explored differences in beta weight modulation of the three stimulation groups measured within the DVAN relative to DMN. An LMM was employed to investigate the effect of tRNS combined with training (Parietal, hMT and Sham condition) and of network (DVAN and DMN) on normalized delta beta weights in response to the OD task (with a random effect for subjects). The analysis revealed significant effects for Condition (χ^2=6.170, df=2, p = 0.046) and a highly significant interaction between Condition and Network (χ^2=23.625, df =2, p < 0.001), while the effect of network alone was not significant (χ^2=2.633, df =1, p = 0.105). Post-hoc analysis using estimated marginal means (EMMs) and pairwise comparisons elucidated the nature of these effects. Notably, pairwise comparisons between networks within each condition indicated that the difference between modulation of beta weights was significant for the Parietal condition (estimate = -0.216, SE = 0.103, p = 0.036 FDR-corrected) and for the Sham condition (estimate = 0.482, SE = 0.103, p < 0.001 FDR-corrected), while no significant difference in beta weights modulation between the two networks was found for the hMT group (estimate = 0.026, SE = 0.099, p = 0.790 FDR-corrected). Differences between networks changes within each stimulation condition are depicted in *Figure 2* (top row).

Next, to further control for changes in the DMN relative to the DVAN, we ran the same LMM to analyze the beta weights relative to the TOJ task. In contrast to the finding for the OD, the results showed that there were no significant effects for Condition (χ^2=1.341, df=2, p = 0.511), nor for network (χ^2=.0004, df=1, p = 0.984), or for the interaction between Condition and Network (χ^2=2.761, p = 0.251). These findings indicate that stimulation had no significant impact on the modulation of beta weights in response to the TOJ task for either the target network (DVAN) or the control network (DMN), nor the interaction between Condition and Network significantly influenced the normalized data (*Figure 2*, bottom row).

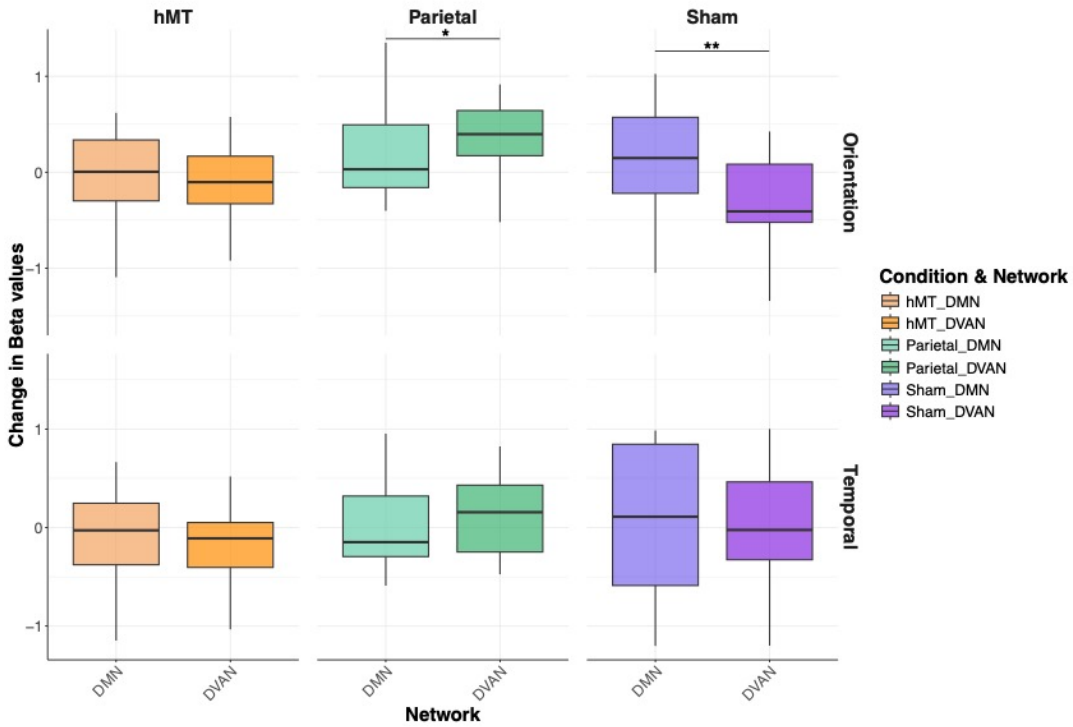

Figure 2. *Box plots for Beta weights changes across conditions (hMT, Parietal and Sham) and networks (DVAN and DMN) in response to the OD (top row) and the TOJ task (bottom row) normalized to baseline and averaged across subjects per stimulation condition. The center line in the middle of the box is the median of each data distribution, while the box represents the interquartile range (IQR), with the lower quartile representing the 25th percentile (Q1) and the upper quartile representing the 75th percentile (Q3). Lines beyond the box represent the minimum and maximum values in the data.*

Impact of stimulation on ROIs' response across conditions

Because the stimulation condition differently influenced the change in beta weights measured between pre and post-test session (expressed as delta) in response to the OD task at a network-level, we aimed to investigate whether stimulation condition exerted differential effects on different ROIs embedded in the DVAN. To this end, we first aimed to understand these effects across all regions of interest without the potential confounding factor of hemispheric lateralization. Indeed, lateralization may affect the functional role of each ROI, potentially leading to differences in responsiveness to stimulation that are unrelated to the intended effects of the task (which is bilateral). An LMM was then fitted to examine the effects of stimulation on normalized delta values across different brain areas regardless of their lateralization, therefore data measured in the left and right hemisphere of each bilateral ROI was collapsed into one ROI. The results revealed significant differences in delta scores across stimulation conditions in several brain regions (*Figure 3A,* left Panel). Specifically, significant main effects of stimulation condition were observed in the hMT (χ^2=19.892, df=2, p = <.001), anterior IPS (χ^2=9.567, df=2, p = 0.008), posterior IPS (χ^2=15.181, df=2, p =.0005), and FEF (χ^2=6.280, df=2, p = .043) regions, while other regions did not show significant changes under different stimulation conditions (see *Table 1* below for detailed statistical results of all models run on each DVAN ROIs). Subsequent post-hoc analyses using estimated marginal means (EMM) further detailed these findings. Pairwise comparisons revealed significant differences between specific conditions in the hMT (Parietal vs. Sham: p <0.001 FDR-corrected, estimate=1.041, t.ratio=4.411; hMT vs. Sham: p=0.017 FDR-corrected, estimate=0.65, t.ratio=2.817) and posterior IPS (Parietal vs. Sham: p<0.001 FDR-corrected, estimate=1.367, t.ratio=3.888) and anterior IPS (Parietal vs. Sham p=0.008 FDR-corrected, estimate =1.122, t.ratio=3.077) regions, indicating robust effects of stimulation condition on delta beta weights relative to the OD task across these brain areas. All other pairwise comparisons were not significant. For the analysis of the brain area anterior TPJ only, we could not fit a *lmer* model as for the other brain areas, because we had only one beta weight per subject (as this region is lateralized to the right); we then used an ANOVA, which was however not significant (F(2,31)=0.224, p=.801).

ROI	ChiSq	Df	Pr(>Chisq)
FEF	6.2806	2	0.0433
hMT	19.8925	2	<.0001
IFJ	3.0996	2	0.2123
IPS	4.5595	2	0.1023
Ant IPS	9.5672	2	0.0084
Post IPS	15.1813	2	0.0005
TPJ	3.9429	2	0.1393
Post TPJ	1.7965	2	0.4073
VFC	4.5445	2	0.1031

Table 1. Results of the LMM for each ROI embedded in the DVAN, with data collapsed across hemispheres for the OD task. For each brain area (left and right hemisphere data were collapsed), *statistical details of the LMM fitted (lmer(normalized* $\Delta\beta$ *~ Condition + (1|subj), data=df_ROI) are reported comprising of Chi-square and corresponding p-value of the model.*

Next, we investigated whether the effects observed are consistent across the network with an analysis that took into consideration each ROI divided per hemisphere. As every single brain area (divided per side) was analyzed independently, and no mixed-linear effects model could be fitted, EMMeans was used to run a series of pairwise comparisons (on delta beta weights) between the stimulation conditions, this time for each of the ROI included in the attentional network divided per hemisphere (*Figure 3B*). This analysis provides estimated marginal means for each combination of the factors "Stimulation" and "ROI", along with confidence intervals and standard errors, and it allows to compare the estimated means between different conditions within each level of brain area (ROI), divided per side. A difference in the change of the beta weights relative to the OD task was found in the following brain areas: in left hMT (parietal vs sham, estimate = 1.378, t.ratio=3.242, *p*=.004 FDR corrected); in left anterior IPS (parietal vs sham, estimate = 1.062, t.ratio=2.498, *p*=0.024 FDR corrected; Parietal vs hMT estimate -1.0075, t.ratio=-2.422, *p*=0.024 FDR-corrected); in right anterior IPS (Parietal vs Sham, estimate=1.183, t.ratio=2.782, *p*=0.017 FDR-corrected), left posterior IPS (Parietal vs Sham, estimate=1.465, t.ratio=3.447, *p*=0.0019 FDR-corrected); right posterior IPS (Parietal vs Sham, estimate=1.268, t.ratio=2.984, *p*=0.009, FDR-corrected). No significant difference between any pair of conditions was instead found for the other ROIs of the attention network. A complete report of all the analysis comparing the delta values for each ROIs divided per hemisphere is reported in the Appendix (*Table 1*,

Appendix). Together, these results suggest that stimulation condition significantly influences neural responses to the OD task across various brain regions, highlighting differential patterns of activation in response to different experimental conditions.

To understand the individual ROI responses to both tasks, we conducted the same analysis on data collected in response to the TOJ task. Consistent with the absence of significance in the main network model, no differences were found between stimulation conditions for any of the ROIs included in the attention network, whether the data was collapsed across hemispheres (*Figure 3A*, right panel) or not (*Figure 3B*, right panel), except for the hMT area, which showed a significant effect only when data were collapsed across hemispheres (χ^2=8.29, df=2, p =0.016). The subsequent pairwise comparison showed a significant increase in BOLD signal within the hMT ROI in comparison to the Sham condition, in the Parietal group only (estimate =0.7, t-ratio= 2.69, p=0.024 FDR- corrected). A complete report of the results relative to the TOJ task are reported in the Appendix (*Table 2* and *Table 3*).

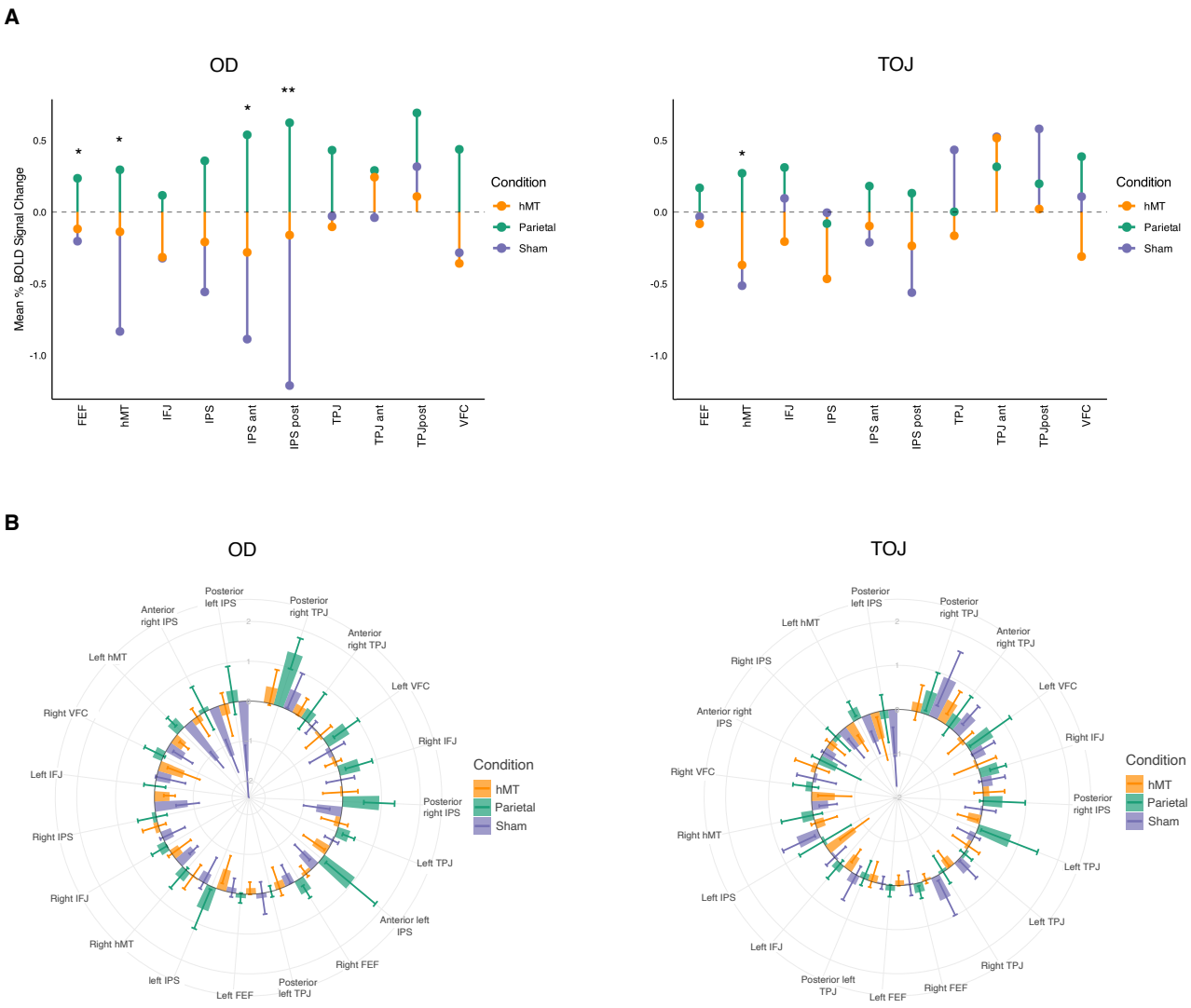

Figure 3. Beta weights changes per single ROI embedded in the DVAN. A. *The lollipop chart illustrates the mean percentage BOLD signal change for each experimental condition and depicted across different brain areas (collapsed across hemisphere, x-axis). Each lollipop segment represents the mean value, lollipop segments above the dashed horizontal line at zero indicate increased BOLD signal, while segments below this line indicate decreased BOLD signal. The chart is facetted by Predictor (OD on the left and TOJ on the right), allowing for comparisons of stimulation conditions within each predictor, as well as between predictors. Asterisks indicate the ROI where there is a significant different BOLD modulation between two or more conditions.* ***B.*** *Changes between pre- and post-test BOLD signal is depicted with bar plots across Conditions (green for Parietal, orange for hMT and violet for Sham) and across tasks (OD on the left and*

TOJ on the right) per each ROI (data were differentiated per hemisphere). The line within each bar indicates the SEM.

Discussion

In this study, we investigated the impact of multi-session tRNS combined with behavioral training on BOLD signal modulation within the attention network (DVAN) during two randomly interleaved attention tasks. Our results indicate that tRNS targeting the bilateral IPS, a critical node of the DVAN, significantly modulated BOLD responses during the orientation discrimination (OD) task, specifically within the main nodes of the attention network. In contrast, no such modulation occurred during the temporal order judgment (TOJ) task, highlighting the task-selective nature of the stimulation effect. Moreover, a control analysis within the default mode network (DMN) showed no significant pre- and post-training changes in any stimulation condition, indicating the network-specific nature of the observed effects.

To date, studies using fMRI to detect functional changes alterations following tES protocols have been almost exclusively focused on tDCS or tACS cortical effects, with very limited exceptions ([50]). Our study is the first to investigate the long-term effects of a multi-session tRNS protocol on cortical dynamics. Our results demonstrate a significant positive modulation of the BOLD signal in the DVAN in response to the OD task following parietal tRNS combined with training. Specifically, participants who received parietal stimulation showed a significant increase in beta weights compared to those who received sham or hMT stimulation. These findings suggest a potential role of tRNS as a network modulator, capable of enhancing neural activity across the attention network when applied to critical nodes such as the IPS. The IPS plays a pivotal role in spatial attention ([56], [57], [58], [59]), and by targeting this key node, tRNS may modulate cortical activity across the network, which likely underlies the observed improvements in task performance (behavioral results are reported in detail in the previous work; [7]). Crucially, stimulation of hMT, did not produce the same effects at either the cortical or behavioral level, further emphasizing the importance of targeting critical regions for significant network-wide modulation.

Moreover, in contrast to the neural activity changes found in response to the OD task, no significant changes in BOLD signal within the DVAN were observed for the TOJ task across the different

stimulation conditions. This suggests that the modulation of neural activity induced by tRNS is also task-specific, possibly reflecting differences in the neural networks engaged by spatial versus temporal processing tasks. The behavioral facilitation observed exclusively in the spatial task ([7]) may indicate that the neural processes supporting spatial attention were prioritized in the context of a cross-training paradigm over those related to temporal processing. Indeed, our experimental paradigm required two different perceptual judgments on the same visual stimuli, which likely induced competition between these representations, ultimately enhancing one while inhibiting the other ([14]), in accordance with the augment Hebbian reweighting model ([60]; see extended discussion on the selective behavioral facilitation in our previous work, [7]). Thus, the behavioral results may reflect this neural task selectivity, further supporting the idea that stimulation combined with training enhances the neural processes that support the visuospatial task. These findings are consistent with a growing body of research suggesting that tES-induced changes have the strongest beneficial effect on behavior when they are task- and network-specific ([43], [61]).

These findings are also consistent with previous tES studies that have found modulation of BOLD responses in targeted cortical regions following tDCS or tACS. For example, Holland and colleagues found that left frontal anodal tDCS had significant behavioral and regional specific neural effects ([52]). Similarly, anodal tDCS over the visual cortex has been found to enhance BOLD responses during visual stimulation tasks, suggesting improved sensory processing ([62]). Studies of tACS have reported increased BOLD signal amplitude in fronto-parietal regions when applied at beta frequencies during both visual and motor tasks, highlighting the influence of tES on network-specific activity ([63]). Although tRNS has been much less studied, Saiote et al. ([50]) reported a reduction in BOLD signal for motor task-related activity in the frontal cortex and precuneus after tRNS application, with no changes after tDCS. However, in this study, stimulation was applied in a single ten-minute session, limiting the assessment of long-term neural changes. Our study is the first to examine the effects of multi-session tRNS on cortical dynamics, providing new insights into how this form of stimulation can modulate neural activity in task-relevant networks.

Interestingly, while we found a significant increase in BOLD signal after parietal stimulation, we also found a significant decrease in the sham condition. Although this decrease is potentially consistent with the neural efficiency (or the neural adaptation) theory, which refers to practice-related decrease in activation as a result of more efficient use of specific neural circuits ([64], [65],

[66]), the decrease in BOLD signal we found is not consistent with the neural efficiency theory, as we did not find any corresponding behavioral improvement in the sham condition ([7]). So, whatever the nature of the reduced hemodynamic signal, it did not benefit behavior. tRNS might have instead maintained or increased neural activity in the parietal regions involved in spatial attention (DVAN), potentially preventing the brain from downregulating its activity and thus promoting learning ([15]). This suggests that tRNS may counteract the natural tendency of the brain to save on neural resources after learning, leading to sustained plasticity and enhanced cognitive functions. We may speculate that tRNS's ability to prevent this adaptive downregulation may stem from its unique stimulation profile. By providing unpredictable, fluctuating electrical inputs, tRNS might interfere with the brain's tendency to stabilize neural activity, thereby maintaining excitability and prolonging plasticity during and after training. Unlike tDCS, where the constant current may induce neuronal adaptation and diminish the potential for sustained enhancement ([67]), tRNS's randomness prevents neurons from habituating to the stimulation, leading to sustained excitability and potentially superior learning outcomes, as shown in our study.

Subsequent analysis involved decomposing the attention network into its constituent components and evaluating the effects of tRNS on beta weights for each region individually. This analysis revealed that the effect of tRNS varied across different ROIs within the DVAN. Notably, significant differences were observed in specific regions of the network: the left hMT, left anterior IPS, right anterior IPS, left posterior IPS, and right posterior IPS exhibited significant increases in delta beta weights following parietal stimulation compared to sham. These findings suggest that parietal tRNS selectively enhances activity in key regions of the DVAN associated with spatial attention, further supporting the role of the IPS in this attentional process and its responsiveness to neuromodulation ([56], [68], [69], [70]). Interestingly, no significant differences were found in other ROIs within the attention network, suggesting that the effect of tRNS may be more robust in specific nodes that are highly task relevant. The region-specific nature of these effects mirrors findings from other studies using techniques such as TMS, tDCS, and tRNS, which have demonstrated that stimulation results are often limited to the most functionally involved nodes ([28], [44], [71], [72]). This selectivity suggests a more targeted effect of this stimulation technique, reinforcing the idea that neuromodulatory interventions should be precisely localized to optimize cognitive outcomes.

Critically, the control analyses performed on the DMN, a network typically active during passive or resting conditions ([55], [73]), showed no significant modulation of the BOLD signal following any stimulation protocol. This lack of changes in the DMN further supports the specificity of our findings within the DVAN, providing compelling evidence that the observed effects are not the result of generalized neural activation but are specifically related to the targeted stimulation and training protocol. This specificity is consistent with previous work showing that the effect of brain stimulation can be limited to targeted networks without affecting unrelated networks ([74], [75]). Furthermore, these results are consistent with our previous functional connectivity analysis, which showed no changes in connectivity patterns within the DMN under similar conditions ([7]).

Notably, these task-related cortical changes found after parietal stimulation are consistent with our previous study evaluating resting-state data from the same experiment, which found increased functional connectivity within the main nodes of the DVAN after parietal stimulation only ([7]). This connectivity pattern correlated with behavioral improvements measured in one of the two attention tasks (OD), suggesting a crucial role for tRNS in modulating network activity that facilitated behavioral improvement in PL. Taken together, these results demonstrate physiological changes indicative of sustained plasticity and behavioral improvement induced by our multi-session training and stimulation protocol, adding to the evidence that tRNS can modulate cortical excitability and improve cognitive functions ([37], [76]).

In summary, the selective enhancement of BOLD responses in the DVAN following parietal tRNS combined with training suggests potential mechanisms of neural plasticity that can be exploited for cognitive enhancement. The significant increase in beta weights in specific ROIs indicates that such protocols may facilitate greater neural engagement and plasticity in cortical regions critical for spatial attention. By integrating targeted cognitive training with optimized stimulation protocols, here we observed increased BOLD responses in critical nodes of the DVAN *during task* performance, and concomitantly stronger functional connectivity *at rest* after training ([7]). These results are consistent with our initial hypothesis and extend the finding of our previous study ([7]). The implications of these findings are relevant to the development of new non-invasive brain stimulation protocols that may promote long-term effects and aim to improve cognitive functions in both healthy individuals and in the clinical populations ([77], [78], [79], [80]).

Conclusion

In conclusion, our study demonstrates that multi-session tRNS targeting the bilateral IPS, combined with task-specific training, selectively enhances BOLD responses in the DVAN during spatial attention tasks. The differential effects across different ROIs within the DVAN highlight the importance of targeting specific brain regions for neuromodulation. These findings underscore the potential of tRNS as a tool for cognitive enhancement and neural plasticity, offering promising avenues for future research and clinical applications.

Material and Methods

Participants

A cohort of thirty-seven neurologically healthy subjects (20 females, mean age 22.8 years old), with normal or corrected-to-normal vision participated in the study. Rigorous screening ensured that all subjects were free of medical contra-indications for both MRI and brain stimulation. Monetary compensation was provided to all participants in acknowledgement of their commitment to the experimental protocol. Ethical approval was obtained from the University of Trento's ethical committee. All Subjects were informed about the nature of the study, potential risks, and benefits, and provided written consent before participating.

Experimental Procedure

Subjects engaged in a comprehensive multi-session experiment that lasted seven days (one session per day; *Figure 4*). On the first session, subjects underwent a staircase procedure that assessed their individual psychophysical thresholds in two attention tasks: an orientation discrimination task (OD), and a temporal order judgment task (TOJ). Both tasks utilized the same visual stimuli consisting of a pair of sine-wave gratings (Gabors, see *Stimuli* section for details). Thresholds for the TOJ and OD tasks were determined separately using 3-1 staircase procedures. Incorrect responses decreased task difficulty, while three consecutive correct responses increased difficulty. The staircases terminated after 30 reversals, and thresholds were calibrated based on these values for the subsequent sessions.

On the second session (pre-test session), participants performed these two attention tasks while in the MRI, with trials of both tasks randomly interleaved within each block. Participants viewed stimuli with fixed temporal offsets (TOJ) and orientation values (OD) set at individual threshold levels determined on the first session. Subjects were cued randomly to attend to either temporal order or orientation feature: each trial began with a 2-second instruction interval where a cue-word ("*Time*" or "*Orientation*") indicated the task for the upcoming trial. Following the cue, stimuli were presented for 500 msec, and subjects made forced-choice judgments during a response interval of 1.5 seconds. The task cue was presented again during the response interval, and the trial concluded with a fixation interval of 2 or 4 seconds. Subjects completed a total of five blocks (corresponding to five MRI scans; see *Neuroimaging Procedures* sections for details).

Subsequent sessions three through six constituted the training and stimulation phase. During these sessions, subjects received 25 minutes hf-tRNS or sham stimulation while concurrently training on the same OD and TOJ tasks. The two trial types were randomly interleaved as the task were presented as in the pre-test. On the last session (post-test session), participants replicated the procedure from the pre-test sessions, performing the OD and TOJ tasks while in the MRI. This comprehensive experimental design allowed for the systematic exploration of the effects of hf-tRNS on attentional tasks.

Stimuli

Visual stimuli employed in the study were identical to those used in our previously published work ([7]), consisting of a pair of sine-wave gratings (Gabors) with fixed temporal offsets and orientation values tailored to individual thresholds. Stimulus presentation and task execution were controlled using Matlab r2016a and Psychtoolbox 3.0.8. For a detailed description of the stimuli used, please refer to the previous work ([7]).

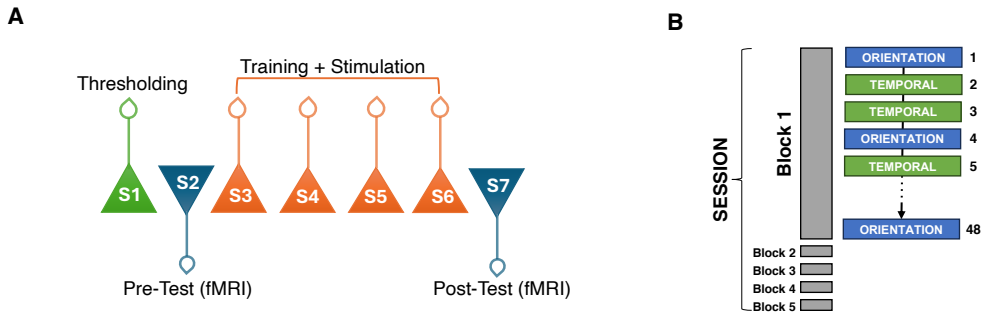

Figure 4. Experimental procedure. A) Experiment Timeline. *On Day 1 subjects underwent the threshold procedure. On Day 2 subjects were tested on the tasks while fMRI data were collected (pre-test session). From Day 3 to Day 6, subjects underwent behavioral training concurrently with tRNS for 25 minutes. Day 7 was a repeat of Day 2 (post-test session).* ***B) Session, with blocks and trials sequence example****. One session comprised 5 blocks: in each block two types of attention tasks (OD and TOJ trials, 48 trials per block for a total of 240 per session) were randomly presented within each block.*

Stimulation Protocol

Participants underwent high-frequency tRNS (hf-tRNS; frequency range 101-640Hz) or sham stimulation targeting specific brain regions, following the international Electroencephalographic 10/20 system for scalp electrode localization ([81]). For hf-tRNS targeting hMT region, electrodes were centered bilaterally over PO7/PO8 (left and right, respectively), while for parietal (IPS) and sham stimulation, electrodes were centered over P3/P4 (*Figure 2*). Stimulation procedure details are described in the previously published work ([7]).

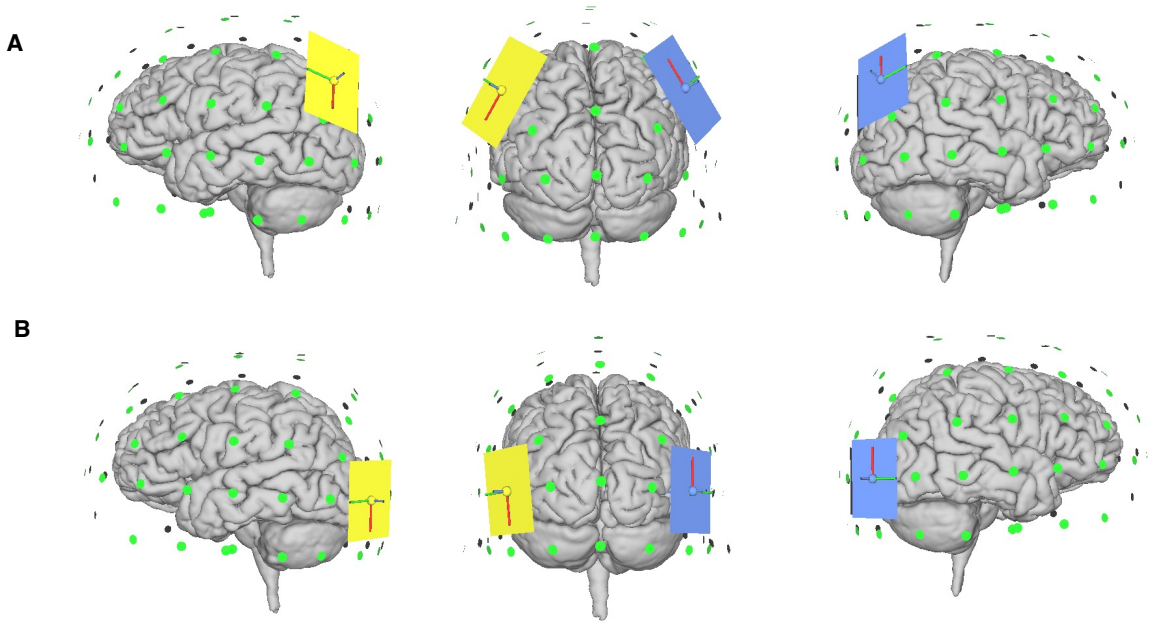

Figure5. Stimulation Settings. *Stimulation sites were localized using the EEG 10/20 system. Electrodes were placed bilaterally over P3 and P4 for Parietal stimulation (Panel A) and for Sham stimulation (Panel A, no active stimulation), and over P07 and P08 for hMT stimulation (Panel B). Images samples were produced using SimNIBS [82], [83]).*

Neuroimaging Procedure (Fast event related fMRI protocol)

Brain imaging sessions were conducted at the Center for Mind and Brain Science of the University of Trento, using a 4T Bruker MedSpec MRI scanner equipped with an 8-channel head-coil. Each session began with the acquisition of high-resolution T1-weighted images (MP-RAGE 1x1x1 mm voxel size, 176 sagittal slices) for anatomical reference. Functional imaging comprised T2*-weighted EPIs (TR=2.0 seconds, TE=28.0, flip angle=73∘, 3x3x3mm voxel size, 0.99mm gap, 30 axial slices acquired interleaved, and a 192 mm FOV) were collected during each session. Each task-related functional run consisted of 185 volumes were acquired, while resting-state functional runs consisted of 120 volumes. Each scanning session included one anatomical run followed by six functional runs (five task runs and one resting-state run performed after every three task runs to allow subjects to rest), lasting approximately one hour.

During functional task runs, we used a Fast Event-Related (FER) fMRI protocol, a neuroimaging experimental design that allows for the investigation of brain responses to individual events or stimuli rapidly presented with a short interstimulus interval (ISI) (Dale 1999; Handwerker et al., 2001). Using a FER fMRI design, we investigated changes in BOLD activity within the primary nodes of the DVAN following multi-session tRNS combined with cognitive training. This analysis would further allow us to assess whether the task-related activity exhibits a similar pattern of results as the resting-state data ([7]).

In each run, subjects viewed either a TOJ or OD trial, presented as a sequential pair of Gabors gratings (see Stimuli section for details) via a periscope mirror mounted on the MR head-coil. Each trial lasted 3.75sec and was followed by a variable ISI (ranging from 2 to 4 seconds). These display presentation parameters are the one used in the previous study published ([7]). No feedback was provided. Stimuli were balanced within each run, such that each type of trial appeared an equal number of times in all five runs. Total number of trials per scanning session was 240 (120 per trial type), for a total of 480 trials per subject (240 for the pre-test session, and 240 for the post-test session). After three blocks, a resting-state scan was acquired. The change in the BOLD signal was assessed by measuring the event-related BOLD response changes pre- and post-test sessions.

Task-related fMRI data analysis

The functional and anatomical data analyses were conducted using BrainVoyager QX (Brain Innovations Inc., Maastricht, The Netherlands). The preprocessing pipeline of the task-related data included the removal of the first 6 volumes to account for non-steady state magnetization (leaving 179 volumes for subsequent analysis), 3D motion correction, slice-timing correction, realignment, and spatial smoothing using a 4mm FWHM Gaussian kernel (full-width at half maximum). Runs with head motion exceeding 3mm in any given dimension were discarded and subjects were eliminated from further analysis when a number equal or greater of 2 runs was excluded in one of the two fMRI sessions (two subjects were eliminated in this step). After preprocessing, the functional scans were initially automatically co-registered and then manually adjusted to each individual's high-resolution anatomical scan. Following co-registration, images were normalized into standardized Talairach coordinates ([84], [85]). A 3D aligned time courses (VTCs) was created for each run after the intra-session anatomical was aligned with the high resolution anatomical.

Next, single-subject deconvolution analysis was performed. We used a deconvolution analysis to analyze the BOLD responses between different stimuli conditions. Beta-weight values over 20-second period following stimulus onset were contrasted within the target processing region. The individual mapping data were subjected to a standard general linear model (GLM) with one predictor for each condition (TOJ and OD) against a rest condition. We then analyzed the deconvolved BOLD response in 19 ROIs included in the DVAN: the right/left anterior, posterior and medial IPS, right/left hMT, right and left frontal eye fields (FEFs) of the dorsal network; the right/left of the posterior, the right anterior and left/right central temporal parietal junction (TPJ), the right/left ventral frontal cortex (VFC), and the right/left inferior frontal junction (IFJ) of the ventral networks. These regions were identified using standardized mean coordinates (*Table 2*) derived from the literature ([8], [21], [51], [86]). Relative to our previous work that investigated functional connectivity within the DVAN ([7]), we included additional ROIs (e.g., IPS was subdivided into posterior, anterior and medial IPS) to better cover the change in activation of the attention network. In fact, this subdivision was important because each region plays a distinct role in attentional processes: the posterior IPS is primarily involved in spatial attention and the integration of visual information ([87]) , while the anterior IPS is associated with the allocation of attentional resources and task relevance ([88]) and the medial IPS is involved in visuospatial attention ([89], [90]). By capturing these differences, we can better understand the varying activation patterns within the attention network and their relationship to behavioral outcomes.

To control for network-specific effects of stimulation, we also investigated whether tRNS and training influenced cortical activity within a different control network, the default mode network (DMN), which is typically active during passive or resting conditions ([55], [91]). The same procedure used for the DVAN analysis was employed to extract the time series and analyze cortical activity within 10 main ROIs of the DMN (same ROIs used in the functional connectivity analysis of the previous work; [7]). These included: the ventral medial prefrontal cortex (vMPFC), the dorsal prefrontal cortex (dPFC), the left posterior cingulate cortex (PCC), the left lateral temporal cortex (TPC), the bilateral inferior parietal lobe (IPL), the bilateral parahippocampal cortex (PHC), and bilateral hippocampal formation (HF+). Coordinates in MNI space were mapped onto Talairach space using the 'MNI-to-Talairach converter with Brodmann Areas tool' included in the Yale BioImage Suite Package ([92]).

Functional data from all voxels within a 4-mm radius sphere from the center coordinate of each ROI were averaged into a single time series, keeping the ROIs similar in size across participants. The time courses were then extracted from each ROI and an individual GLM was applied to estimate the response amplitude, independently for each subject. The resulting beta weights estimate peak activation for each run, assuming a standard 2γ model of the hemodynamic response function. These estimates (peak of the beta weights) from each individual ROI were used as the input to the subsequent statistical analysis.

	LEFT HEMISPHERE			RIGHT HEMISPHERE		
	X	Y	Z	X	Y	Z
IPS	-26	-63	48	25	-60	48
Anterior IPS	-25	-55	50	25	-59	56
Posterior IPS	-19	-63	60	17	-65	54
hMT	-44	-67	3	44	-71	6
FEF	-30	-5	48	30	-5	48
TPJ	-48	-54	26	48	-54	21
VFC	-42	12	-1	40	17	4
Anterior TPJ				54	-41	28
Posterior TPJ	-44	-66	22	49	-61	20
IFJ	-40	7	25	44	12	27

Table 2. Regions of Interest Coordinates*. Standardized Talairach coordinates (X,Y,Z) for the centroid of each region of interest (Left and Right hemisphere) for the DVAN.*

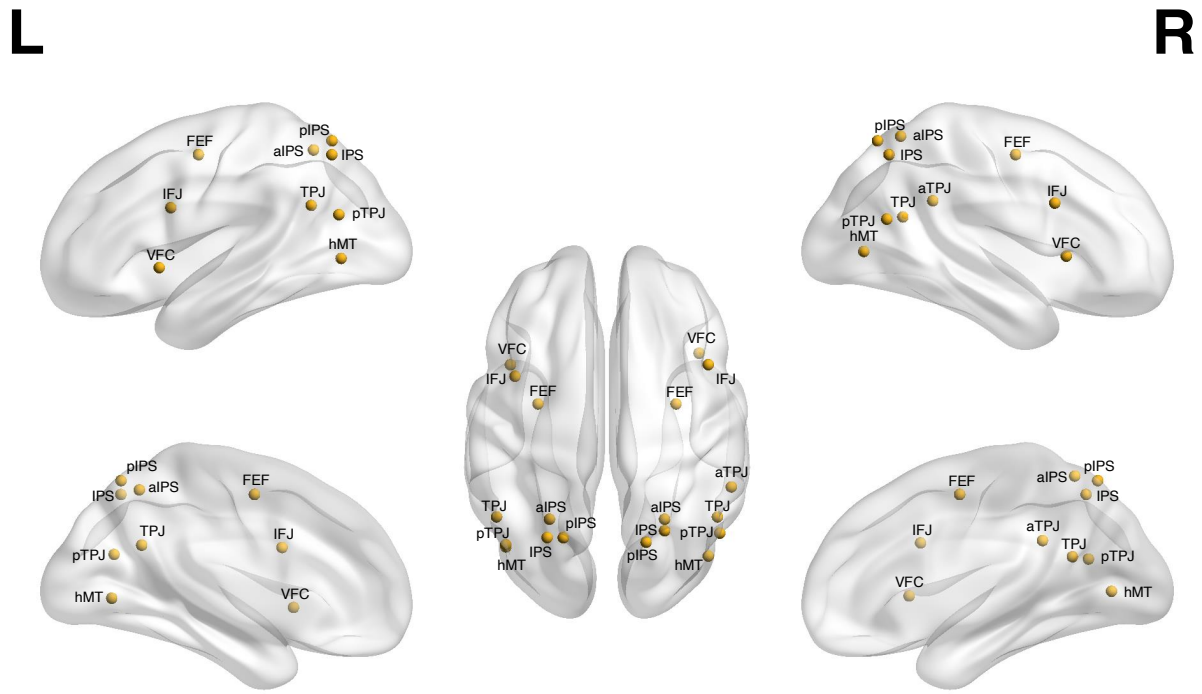

Figure 6. *Brain representation of the ROIs embedded in the attention network. Three-dimensioned views (sagittal and coronal views) of the ROI spheres embedded in the attention network, visualized with BrainNet Viewer package for visualization ([93]).*

Data Analysis

We conducted an analysis of BOLD signal changes in response to attentional tasks, specifically the OD and the TOJ task. Peaks of the beta weights relative to individual ROI collected during pre- and post-stimulation fMRI session (pre- and post-sessions) were analyzed. To evaluate the impact of stimulation combined with training on the attentional network, we calculated beta weights representing the overall modulation of the DVAN. These beta weights were derived within each ROI first and then averaged across ROIs to obtain a single beta weight per subject, reflecting the overall trend in BOLD signal modulation ([94]).

First, to assess baseline comparability between stimulation groups prior to stimulation (at baseline), we conducted a linear mixed-effects model using *lmer*() function from the lme4 package ([95]) in RStudio (version 2023.06.0). Next, delta scores representing the difference between pre- and post-stimulation beta weights were computed on individual subject ($\Delta\beta = \beta$(fMRI post-test)–β(fMRI pre-test) to quantify changes in BOLD signal modulation. These delta measures reflect the stimulation-induced changes in BOLD signal normalized to baseline. Within-subject delta beta weights were derived to capture the individualized BOLD modulation rather than a group average approach

([96], [97]; for further discussion about differences between within-subjects versus group-averaged approaches, see [98]). A mixed effects model was then fit on subjects' delta beta weights, where the between-subjects predictor was Stimulation (Parietal, hMT, Sham), and the within-subjects predictor was Task (OD and TOJ). Model comparisons were conducted, and the selected model formula was *lmer*($\Delta\beta$ ~ Stimulation*Task+(1+session|subject), data = df_delta_betas). This linear mixed-effects model was based on the delta scores, and random intercepts and slopes were included for each subject. Chi-squared and p-values were reported for both interactions and main effects. After fitting a linear mixed-effects model, estimated marginal means (EMMs) were computed for each level of the stimulation factor. Contrasts between stimulation levels were then estimated, and associated standard errors, confidence intervals, t-ratios, and p-values were

calculated. Adjustments for multiple comparisons were made using the FDR method ([99]). The same statistical analyses were then computed on the beta weights of the main ROIs included in DMN to examine whether stimulation and training induced changes in cortical activity in this control network.

Finally, we compared the change in beta values measured within the DVAN and the DMN. A mixed-effects model was fitted on subjects' delta beta scores of both networks, with network (DVAN and DMN) and task (OD and TOJ) serving as the within-subject predictor and stimulation (Parietal, hMT, Sham) as the between-subjects predictor. This model served to evaluate whether there was a difference in signal modulation within the two networks depending on stimulation conditions, hence indicating whether stimulation affected a specific network or was general in the whole brain.

References

[1] R. L. Goldstone, "Perceptual learning.," *Annu Rev Psychol*, vol. 49, pp. 585–612, 1998.

[2] C. D. Gilbert, "Learning. Neuronal dynamics and perceptual learning.," *Curr Biol*, vol. 4, no. 7, pp. 627–9, Jul. 1994, doi: 10.1016/s0960-9822(00)00138-x.

[3] T. Watanabe and Y. Sasaki, "Perceptual Learning: Toward a Comprehensive Theory," *Annu Rev Psychol*, vol. 66, no. 1, pp. 197–221, 2015, doi: 10.1146/annurev-psych-010814-015214.

[4] Y. Sasaki, J. E. Nanez, and T. Watanabe, "Advances in visual perceptual learning and plasticity," *Nat Rev Neurosci*, vol. 11, no. 1, pp. 53–60, 2009.

[5] K. Shibata, Y. Sasaki, M. Kawato, and T. Watanabe, "Neuroimaging Evidence for 2 Types of Plasticity in Association with Visual Perceptual Learning," *Cereb. Cortex*, vol. 26, no. 9, pp. 3681–3689, 2016, doi: 10.1093/cercor/bhw176.

[6] C. D. Gilbert, W. Li, and V. Piech, "Perceptual learning and adult cortical plasticity," *J Physiol*, vol. 587, no. 12, pp. 2743–2751, Jun. 2009, doi: 10.1113/jphysiol.2009.171488.

[7] F. Contò, G. Edwards, S. Tyler, D. Parrott, E. Grossman, and L. Battelli, "Attention network modulation via tRNS correlates with attention gain," *Elife*, vol. 10, Nov. 2021, doi: 10.7554/eLife.63782.

[8] S. Vossel, J. J. Geng, and G. R. Fink, "Dorsal and Ventral Attention Systems," *The Neuroscientist*, vol. 20, no. 2, pp. 150–159, Apr. 2014, doi: 10.1177/1073858413494269.

[9] S. Vossel, J. J. Geng, and G. R. Fink, "Dorsal and ventral attention systems: Distinct neural circuits but collaborative roles," *Neuroscientist*, vol. 20, no. 2, pp. 150–159, 2014, doi: 10.1177/1073858413494269.

[10] M. I. Posner, "Imaging attention networks," *Neuroimage*, vol. 61, no. 2, pp. 450–456, Jun. 2012, doi: 10.1016/J.NEUROIMAGE.2011.12.040.

[11] I. Mukai, D. Kim, M. Fukunaga, S. Japee, S. Marrett, and L. G. Ungerleider, "Activations in Visual and Attention-Related Areas Predict and Correlate with the Degree of Perceptual Learning," *J. Neurosci.*, vol. 27, no. 42, pp. 11401–11411, 2007, doi: 10.1523/JNEUROSCI.3002-07.2007.

[12] Y. Yotsumoto and T. Watanabe, "Defining a link between perceptual learning and attention.," *PLoS Biol*, vol. 6, no. 8, p. e221, Aug. 2008, doi: 10.1371/journal.pbio.0060221.

[13] S. F. A. Szpiro and M. Carrasco, "Exogenous Attention Enables Perceptual Learning," *Psychol Sci*, 2015, doi: 10.1177/0956797615598976.

[14] F. Contò, S. Tyler, P. Paletta, and L. Battelli, "The role of the parietal lobe in task-irrelevant suppression during learning," *Brain Stimul*, vol. 16, pp. 715–723, 2023, doi: 10.1016/j.brs.2023.04.006.

[15] G. Edwards, F. Contò, L. K. Bucci, and L. Battelli, "Controlling Brain State Prior to Stimulation of Parietal Cortex Prevents Deterioration of Sustained Attention," *Cereb Cortex Commun*, vol. 1, pp. 1–13, 2020, doi: 10.1093/texcom/tgaa069.

[16] W. Li, V. Piëch, and C. D. Gilbert, "Perceptual learning and top-down influences in primary visual cortex.," *Nat Neurosci*, vol. 7, no. 6, pp. 651–657, 2004.

[17] R. E. Crist, W. Li, and C. D. Gilbert, "Learning to see: experience and attention in primary visual cortex," *Nat Neurosci*, vol. 4, no. 5, pp. 519–525, May 2001, doi: 10.1038/87470.

[18] P. R. Roelfsema, A. van Ooyen, and T. Watanabe, "Perceptual learning rules based on reinforcers and attention," *Trends Cogn Sci*, vol. 14, no. 2, p. 64, Feb. 2010, doi: 10.1016/J.TICS.2009.11.005.

[19] S. C. Tyler, S. Dasgupta, S. Agosta, L. Battelli, and E. D. Grossman, "Functional connectivity of parietal cortex during temporal selective attention," *Cortex*, vol. 65, pp. 195–207, 2015, doi: 10.1016/j.cortex.2015.01.015.

[20] M. Corbetta and G. L. Shulman, "Control of goal-directed and stimulus-driven attention in the brain," *Nat Rev Neurosci*, vol. 3, no. 3, pp. 201–215, 2002, doi: 10.1038/nrn755.

[21] M. Corbetta, G. Patel, and G. L. Shulman, "The Reorienting System of the Human Brain: From Environment to Theory of Mind," *Neuron*, vol. 58, no. 3, p. 306, May 2008, doi: 10.1016/J.NEURON.2008.04.017.

[22] M. T. De Schotten *et al.*, "A lateralized brain network for visuospatial attention," *Nat Neurosci*, vol. 14, no. 10, pp. 1245–1246, Oct. 2011, doi: 10.1038/NN.2905.

[23] P. G. Allan *et al.*, "Parcellation-based tractographic modeling of the dorsal attention network," *Brain Behav*, vol. 9, no. 10, p. e01365, Oct. 2019, doi: 10.1002/BRB3.1365.

[24] I. Sani, B. C. McPherson, H. Stemmann, F. Pestilli, and W. A. Freiwald, "Functionally defined white matter of the macaque monkey brain reveals a dorso-ventral attention network," *Elife*, vol. 8, Jan. 2019, doi: 10.7554/eLife.40520.

[25] M. D. Greicius, B. Krasnow, A. L. Reiss, and V. Menon, "Functional connectivity in the resting brain: A network analysis of the default mode hypothesis," *Proc Natl Acad Sci U S A*, vol. 100, no. 1, pp. 253–258, 2003, doi: 10.1073/pnas.0135058100.

[26] X. Suo *et al.*, "Anatomical and functional coupling between the dorsal and ventral attention networks," *Neuroimage*, vol. 232, p. 117868, May 2021, doi: 10.1016/J.NEUROIMAGE.2021.117868.

[27] C. Pirulli, A. Fertonani, and C. Miniussi, "Brain Stimulation The Role of Timing in the Induction of Neuromodulation in Perceptual Learning by Transcranial Electric Stimulation," *Brain Stimul*, vol. 6, no. 4, pp. 683–689, 2013, doi: 10.1016/j.brs.2012.12.005.

[28] F. Herpich, M. D. Melnick, S. Agosta, K. R. Huxlin, D. Tadin, and L. Battelli, "Boosting Learning Efficacy with Noninvasive Brain Stimulation in Intact and Brain-Damaged Humans," *The Journal of Neuroscience*, vol. 39, no. 28, pp. 5551 LP – 5561, Jul. 2019, doi: 10.1523/JNEUROSCI.3248-18.2019.

[29] a. Fertonani, C. Pirulli, and C. Miniussi, "Random Noise Stimulation Improves Neuroplasticity in Perceptual Learning," *Journal of Neuroscience*, vol. 31, no. 43, pp. 15416–15423, 2011, doi: 10.1523/JNEUROSCI.2002-11.2011.

[30] M. Cappelletti *et al.*, "Transfer of Cognitive Training across Magnitude Dimensions Achieved with Concurrent Brain Stimulation of the Parietal Lobe," *J. Neurosci.*, vol. 33, no. 37, pp. 14899–14907, 2013, doi: 10.1523/JNEUROSCI.1692-13.2013.

[31] M. A. Nitsche and W. Paulus, "Transcranial direct current stimulation--update 2011," *Restor Neurol Neurosci*, vol. 29, no. 6, pp. 463–492, 2011, doi: 10.3233/RNN-2011-0618.

[32] S. Bestmann and V. Walsh, "Transcranial electrical stimulation," *Curr. Biol.*, vol. 27, no. 23, pp. R1258–R1262, 2017. doi: 10.1016/j.cub.2017.11.001.

[33] I. Moreno-duarte, N. Gebodh, B. Guleyupoglu, D. Reato, M. Bikson, and F. Fregni, *Transcranial Electrical Stimulation : Transcranial Direct Current Stimulation (tDCS), Noise Stimulation (tRNS)*. Elsevier Inc., 2014. doi: 10.1016/B978-0-12-404704-4.00002-8.

[34] F. Fröhlich and D. A. McCormick, "Endogenous Electric Fields May Guide Neocortical Network Activity," *Neuron*, vol. 67, no. 1, p. 129, Jul. 2010, doi: 10.1016/J.NEURON.2010.06.005.

[35] D. Reato, A. Rahman, M. Bikson, and L. C. Parra, "Low-Intensity Electrical Stimulation Affects Network Dynamics by Modulating Population Rate and Spike Timing," *The Journal of Neuroscience*, vol. 30, no. 45, p. 15067, Nov. 2010, doi: 10.1523/JNEUROSCI.2059-10.2010.

[36] M. R. Krause, T. P. Zanos, B. A. Csorba, M. E. Phillips, A. Datta, and C. C. Pack, "Transcranial Direct Current Stimulation Facilitates Associative Learning and Alters Functional Connectivity in the Primate Brain," *Current Biology*, vol. 27, pp. 3086-3096.e3, 2017, doi: 10.1016/j.cub.2017.09.020.

[37] A. Fertonani and C. Miniussi, "Transcranial Electrical Stimulation : What We Know and Do Not Know About Mechanisms," *Neuroscientist*, vol. 23, no. 2, pp. 109–123, 2017, doi: 10.1177/1073858416631966.

[38] A. Pecchinenda *et al.*, "Contributions of the right prefrontal and parietal cortices to the attentional blink: A tdcs study," *Symmetry*, vol. 13, no. 7, p. 1208, 2021, doi: 10.3390/sym13071208.

[39] A. Pavan, F. Ghin, A. Contillo, C. Milesi, G. Campana, and G. Mather, "Modulatory mechanisms underlying high-frequency transcranial random noise stimulation (hf-tRNS): A combined stochastic resonance and equivalent noise approach," *Brain Stimul*, vol. 12, no. 4, pp. 967–977, Jul. 2019, doi: 10.1016/J.BRS.2019.02.018.

[40] B. Moret *et al.*, "Differential effects of high-frequency transcranial random noise stimulation (hf-tRNS) on contrast sensitivity and visual acuity when combined with a short perceptual training in adults with amblyopia," *Neuropsychologia*, vol. 114, pp. 125–133, Jun. 2018, doi: 10.1016/j.neuropsychologia.2018.04.017.

[41] F. Herpich, F. Contò, M. van Koningsbruggen, and L. Battelli, "Modulating the excitability of the visual cortex using a stimulation priming paradigm," *Neuropsychologia*, vol. 119, pp. 165–171, Oct. 2018, doi: 10.1016/J.NEUROPSYCHOLOGIA.2018.08.009.

[42] A. Fertonani, C. Pirulli, and C. Miniussi, "Random Noise Stimulation Improves Neuroplasticity in Perceptual Learning," *Journal of Neuroscience*, vol. 31, no. 43, pp. 15416–15423, 2011.

[43] C. Pirulli, A. Fertonani, and C. Miniussi, "The role of timing in the induction of neuromodulation in perceptual learning by transcranial electric stimulation," *Brain Stimul*, vol. 6, no. 4, pp. 683–689, 2013.

[44] S. C. Tyler, F. Contò, and L. Battelli, "Rapid Improvement on a Temporal Attention Task within a Single Session of High-frequency Transcranial Random Noise Stimulation," *J Cogn Neurosci*, vol. 30, no. 5, pp. 656–666, May 2018, doi: 10.1162/jocn_a_01235.

[45] O. van der Groen and N. Wenderoth, "Transcranial Random Noise Stimulation of Visual Cortex: Stochastic Resonance Enhances Central Mechanisms of Perception.," *The Journal of neuroscience*, vol. 36, no. 19, pp. 5289–5298, 2016.

[46] G. Prete, A. D'Anselmo, L. Tommasi, and A. Brancucci, "Modulation of the dichotic right ear advantage during bilateral but not unilateral transcranial random noise stimulation," *Brain Cogn*, vol. 123, pp. 81–88, Jun. 2018, doi: 10.1016/J.BANDC.2018.03.003.

[47] Y. Inukai, K. Saito, R. Sasaki, S. Tsuiki, and S. Miyaguchi, "Comparison of Three Non-Invasive Transcranial Electrical Stimulation Methods for Increasing Cortical Excitability," *Front. Hum. Neurosci.*, vol. 10, p. 668, 2016, doi: 10.3389/fnhum.2016.00668.

[48] V. Moliadze, G. Fritzsche, and A. Antal, "Comparing the Efficacy of Excitatory Transcranial Stimulation Methods Measuring Motor Evoked Potentials," *Neural Plast.*, vol. 2014, no. 1, p. 837141, 2014, doi: 10.1155/2014/837141.

[49] O. Van Der Groen, W. Potok, N. Wenderoth, G. Edwards, J. B. Mattingley, and D. Edwards, "Using noise for the better: The effects of transcranial random noise stimulation on the brain and behavior," *Neurosci. Biobehav. Rev.*, vol. 138, p. 104702, 2022, doi: 10.1016/j.neubiorev.2022.104702.

[50] C. Saiote, R. Polanía, K. Rosenberger, W. Paulus, and A. Antal, "High-Frequency TRNS Reduces BOLD Activity during Visuomotor Learning," *PLoS One*, vol. 8, no. 3, p. 59669, 2013, doi: 10.1371/journal.pone.0059669.

[51] L. Battelli, E. D. Grossman, and E. B. Plow, "Brain Stimulation Local Immediate versus Long-Range Delayed Changes in Functional Connectivity Following rTMS on the Visual Attention Network," *Brain Stimul*, vol. 10, no. 2, pp. 263–269, 2017, doi: 10.1016/j.brs.2016.10.009.

[52] R. Holland *et al.*, "Speech facilitation by left inferior frontal cortex stimulation," *Curr Biol*, vol. 21, no. 16, pp. 1403–1407, Aug. 2011, doi: 10.1016/J.CUB.2011.07.021.

[53] M. E. Raichle, A. M. MacLeod, A. Z. Snyder, W. J. Powers, D. A. Gusnard, and G. L. Shulman, "A default mode of brain function," *Proc Natl Acad Sci U S A*, vol. 98, no. 2, pp. 676–682, 2001, doi: 10.1073/pnas.98.2.676.

[54] R. L. Buckner, J. R. Andrews-Hanna, and D. L. Schacter, "The brain's default network: Anatomy, function, and relevance to disease," *Ann N Y Acad Sci*, vol. 1124, pp. 1–38, 2008, doi: 10.1196/annals.1440.011.

[55] R. L. Buckner and L. M. DiNicola, "The brain's default network: updated anatomy, physiology and evolving insights," *Nat Rev Neurosci*, vol. 20, no. 10, pp. 593–608, 2019, doi: 10.1038/s41583-019-0212-7.

[56] P. Capotosto, C. Babiloni, G. L. Romani, and M. Corbetta, "Frontoparietal Cortex Controls Spatial Attention through Modulation of Anticipatory Alpha Rhythms," *Journal of Neuroscience*, vol. 29, no. 18, pp. 5863–5872, May 2009, doi: 10.1523/JNEUROSCI.0539-09.2009.

[57] E. B. Plow, Z. Cattaneo, T. A. Carlson, G. A. Alvarez, A. Pascual-Leone, and L. Battelli, "The compensatory dynamic of inter-hemispheric interactions in visuospatial attention revealed using rTMS and fMRI," *Front Hum Neurosci*, vol. 8, no. 1 APR, p. 81300, Apr. 2014, doi: 10.3389/FNHUM.2014.00226/BIBTEX.

[58] P. Capotosto, M. Corbetta, G. L. Romani, and C. Babiloni, "Electrophysiological Correlates of Stimulus-driven Reorienting Deficits after Interference with Right Parietal Cortex during a Spatial Attention Task: A TMS-EEG Study," *J. Cogn. Neurosci.*, vol. 24, no. 12, pp. 2363–2371, 2012, doi: https://doi.org/10.1162/jocn_a_00287.

[59] M. Corbetta and G. L. Shulman, "Spatial Neglect and Attention Networks," *Annu. Rev. Neurosci.*, vol. 34, no. 1, pp. 569–599, 2011, doi: 10.1146/ANNUREV-NEURO-061010-113731.

[60] B. A. Dosher, P. Jeter, J. Liu, and Z.-L. Lu, "An integrated reweighting theory of perceptual learning.," *Proc Natl Acad Sci U S A*, vol. 110, no. 33, pp. 13678–83, Aug. 2013, doi: 10.1073/pnas.1312552110.

[61] E. Santarnecchi, A. K. Brem, E. Levenbaum, T. Thompson, R. C. Kadosh, and A. Pascual-Leone, "Enhancing cognition using transcranial electrical stimulation," *Curr Opin Behav Sci*, vol. 4, pp. 127–178, 2015, doi: 10.1016/j.cobeha.2015.06.003.

[62] I. Alekseichuk, K. Diers, W. Paulus, and A. Antal, "Transcranial electrical stimulation of the occipital cortex during visual perception modifies the magnitude of BOLD activity: A combined tES–fMRI approach," *Neuroimage*, vol. 140, pp. 110–117, Oct. 2016, doi: 10.1016/J.NEUROIMAGE.2015.11.034.

[63] Y. Cabral-Calderin *et al.*, "Transcranial alternating current stimulation affects the BOLD signal in a frequency and task-dependent manner," *Hum Brain Mapp*, vol. 37, no. 1, pp. 94–121, Jan. 2016, doi: 10.1002/HBM.23016.

[64] A. M. C. Kelly and H. Garavan, "Human Functional Neuroimaging of Brain Changes Associated with Practice," *Cerebral Cortex*, vol. 15, no. 8, pp. 1089–1102, Aug. 2005, doi: 10.1093/CERCOR/BHI005.

[65] Y. Yotsumoto, T. Watanabe, and Y. Sasaki, "Different dynamics of performance and brain activation in the time course of perceptual learning," *Neuron*, vol. 57, no. 6, pp. 827–833, Mar. 2008, doi: 10.1016/J.NEURON.2008.02.034.

[66] D. Sagi, "Perceptual learning in Vision Research," *Vis. Res.*, vol. 51, no. 13, pp. 1552–1566, 2011, doi: 10.1016/j.visres.2010.10.019.

[67] K. Fricke, A. A. Seeber, N. Thirugnanasambandam, W. Paulus, M. A. Nitsche, and J. C. Rothwell, "Time course of the induction of homeostatic plasticity generated by repeated transcranial direct current stimulation of the human motor cortex," *J Neurophysiol*, vol. 105, no. 3, pp. 1141–1149, Mar. 2011, doi: 10.1152/JN.00608.2009.

[68] P. Capotosto *et al.*, "Anatomical segregation of visual selection mechanisms in human parietal cortex.," *J Neurosci*, vol. 33, no. 14, pp. 6225–9, Apr. 2013, doi: 10.1523/JNEUROSCI.4983-12.2013.

[69] C. Grefkes and G. R. Fink, "The functional organization of the intraparietal sulcus in humans and monkeys," *J Anat*, vol. 207, no. 1, p. 3, Jul. 2005, doi: 10.1111/J.1469-7580.2005.00426.X.

[70] L. Brown, L. K. White, W. Makhoul, M. Teferi, Y. I. Sheline, and N. L. Balderston, "Role of the intraparietal sulcus (IPS) in anxiety and cognition: Opportunities for intervention for anxiety-related disorders," *International Journal of Clinical and Health Psychology*, vol. 23, no. 4, p. 100385, Oct. 2023, doi: 10.1016/J.IJCHP.2023.100385.

[71] G. Edwards *et al.*, "Prolonged neuromodulation of cortical networks following low-frequency rTMS and its potential for clinical interventions," *Front Psychol*, vol. 10, no. MAR, p. 529, 2019, doi: 10.3389/FPSYG.2019.00529/BIBTEX.

[72] F. Yavari, A. Jamil, M. Mosayebi Samani, L. P. Vidor, and M. A. Nitsche, "Basic and functional effects of transcranial Electrical Stimulation (tES)—An introduction," *Neurosci Biobehav Rev*, vol. 85, pp. 81–92, Feb. 2018, doi: 10.1016/J.NEUBIOREV.2017.06.015.

[73] R. L. Buckner, "The serendipitous discovery of the brain's default network," *Neuroimage*, vol. 62, no. 2, pp. 1137–1145, 2012, doi: 10.1016/j.neuroimage.2011.10.035.

[74] T. Neuling, S. Rach, and C. S. Herrmann, "Orchestrating neuronal networks: sustained after-effects of transcranial alternating current stimulation depend upon brain states," *Front Hum Neurosci*, vol. 7, p. 161, Apr. 2013, doi: 10.3389/fnhum.2013.00161.

[75] M. Meinzer, R. Lindenberg, D. Antonenko, T. Flaisch, and A. Flöel, "Anodal Transcranial Direct Current Stimulation Temporarily Reverses Age-Associated Cognitive Decline and Functional Brain Activity Changes," *Journal of Neuroscience*, vol. 33, no. 30, pp. 12470–12478, Jul. 2013, doi: 10.1523/JNEUROSCI.5743-12.2013.

[76] D. Terney, L. Chaieb, V. Moliadze, A. Antal, and W. Paulus, "Increasing Human Brain Excitability by Transcranial High- Frequency Random Noise Stimulation," *J. Neurosci.*, vol. 28, no. 52, pp. 14147–14155, 2008, doi: 10.1523/JNEUROSCI.4248-08.2008.

[77] R. Polanía, M. A. Nitsche, and C. C. Ruff, "Establishing brain-behavior relations with NIBS Studying and modifying brain function with non-invasive brain stimulation," *Nat Neurosci*, vol. 21, pp. 174–187, 2018, doi: 10.1038/s41593-017-0054-4.

[78] B. A. Coffman, V. P. Clark, and R. Parasuraman, "Battery powered thought: Enhancement of attention, learning, and memory in healthy adults using transcranial direct current stimulation," *Neuroimage*, vol. 85, pp. 895–908, Jan. 2014, doi: 10.1016/J.NEUROIMAGE.2013.07.083.

[79] H. Meng, M. Houston, Y. Zhang, and S. Li, "Exploring the Prospects of Transcranial Electrical Stimulation (tES) as a Therapeutic Intervention for Post-Stroke Motor Recovery: A Narrative Review," *Brain Sciences 2024, Vol. 14, Page 322*, vol. 14, no. 4, p. 322, Mar. 2024, doi: 10.3390/BRAINSCI14040322.

[80] Y. Lv *et al.*, "A meta-analysis of the effects of transcranial direct current stimulation combined with cognitive training on working memory in healthy older adults," *Front Aging Neurosci*, vol. 16, p. 1454755, Sep. 2024, doi: 10.3389/FNAGI.2024.1454755.

[81] U. Herwig, P. Satrapi, and C. Schönfeldt-Lecuona, "Using the International 10-20 EEG System for Positioning of Transcranial Magnetic Stimulation," *Brain Topogr*, vol. 16, no. 2, pp. 95–99, Dec. 2003, doi: 10.1023/B:BRAT.0000006333.93597.9D/METRICS.

[82] A. Thielscher, A. Antunes, and G. B. Saturnino, "Field modeling for transcranial magnetic stimulation: A useful tool to understand the physiological effects of TMS?," in *2015 37th Annual International Conference of the IEEE Engineering in Medicine and Biology Society (EMBC)*, IEEE, Aug. 2015, pp. 222–225. doi: 10.1109/EMBC.2015.7318340.

[83] G. B. Saturnino, O. Puonti, J. D. Nielsen, D. Antonenko, K. H. Madsen, and A. Thielscher, "SimNIBS 2.1: A Comprehensive Pipeline for Individualized Electric Field Modelling for Transcranial Brain Stimulation," *Brain and Human Body Modeling: Computational Human Modeling at EMBC 2018*, pp. 3–25, Aug. 2019, doi: 10.1007/978-3-030-21293-3_1.

[84] L. Laitinen, "Co-planar stereotaxic atlas of the human brain: 3-dimensional proportional system: an approach to cerebral imaging. By Jean Talairach and Pierre Tournoux. Translated by Mark Rayport. Georg Thieme Verlag, Stuttgart-New York, 1988. pp. 122). ISBN 313711701-1 (Georg Thieme Verlag, Stuttgart; ISBN 0 86577 293 2 (Thieme Medical Publishers, Inc. New York)," *Clin Neurol Neurosurg*, vol. 91, no. 3, pp. 277–278, Jan. 1989, doi: 10.1016/0303-8467(89)90128-5.

[85] "Talairach J, Tournoux P. 1988 Co-planar stereotaxic atlas of the human brain. Clinical Neurology and Neurosurgery 91: 277–278. DOI: https://doi.org/10.1016/0303-8467(89)90128-5

[86] M. D. Fox, M. Corbetta, A. Z. Snyder, J. L. Vincent, and M. E. Raichle, "Spontaneous neuronal activity distinguishes human dorsal and ventral attention systems.," *Proc Natl Acad Sci U S A*, vol. 103, no. 26, pp. 10046–51, Jun. 2006, doi: 10.1073/pnas.0604187103.

[87] J. C. Culham and N. G. Kanwisher, "Neuroimaging of cognitive functions in human parietal cortex," *Curr Opin Neurobiol*, vol. 11, no. 2, pp. 157–163, Apr. 2001, doi: 10.1016/S0959-4388(00)00191-4.

[88] J. J. Geng and G. R. Mangun, "Anterior intraparietal sulcus is sensitive to bottom-up attention driven by stimulus salience," *J Cogn Neurosci*, vol. 21, no. 8, pp. 1584–1601, Aug. 2009, doi: 10.1162/JOCN.2009.21103.

[89] R. A. Andersen, "Encoding of Intention and Spatial Location in the Posterior Parietal Cortex," *Cerebral Cortex*, vol. 5, no. 5, pp. 457–469, Sep. 1995, doi: 10.1093/CERCOR/5.5.457.

[90] L. H. Snyder, A. P. Batista, and R. A. Andersen, "Intention-related activity in the posterior parietal cortex: a review," *Vis. Res.*, vol. 40, no. 10-12, pp. 1433–1441, 2000, doi: https://doi.org/10.1016/S0042-6989(00)00052-3

[91] M. E. Raichle, "The Brain's Default Mode Network," *Annu Rev Neurosci*, vol. 38, no. April, pp. 433–447, 2015, doi: 10.1146/annurev-neuro-071013-014030.

[92] X. Papademetris, M. Jackowski, N. Rajeevan, R. T. Constable, and L. Staib, "BioImage Suite: An integrated medical image analysis suite," *Insight J*, Jan. 2022, doi: 10.54294/VB5Z20.

[93] M. Xia, J. Wang, and Y. He, "BrainNet Viewer: A Network Visualization Tool for Human Brain Connectomics," *PLoS One*, vol. 8, no. 7, Jul. 2013, doi: 10.1371/journal.pone.0068910.

[94] M. P. van den Heuvel, S. C. de Lange, A. Zalesky, C. Seguin, B. T. T. Yeo, and R. Schmidt, "Proportional thresholding in resting-state fMRI functional connectivity networks and consequences for patient-control connectome studies: Issues and recommendations," *Neuroimage*, vol. 152, pp. 437–449, May 2017, doi: 10.1016/J.NEUROIMAGE.2017.02.005.

[95] D. Bates, M. Mächler, E. Zurich, B. M. Bolker, and S. C. Walker, "Fitting linear mixed-effects models using lme4".

[96] E. Varangis, C. G. Habeck, Q. R. Razlighi, and Y. Stern, "The Effect of Aging on Resting State Connectivity of Predefined Networks in the Brain," *Front Aging Neurosci*, vol. 11, no. September, 2019, doi: 10.3389/fnagi.2019.00234.

[97] B. Bellana, Z. X. Liu, N. B. Diamond, C. L. Grady, and M. Moscovitch, "Similarities and differences in the default mode network across rest, retrieval, and future imagining," *Hum Brain Mapp*, vol. 38, no. 3, pp. 1155–1171, 2017, doi: 10.1002/hbm.23445.

[98] R. P. Roberts, S. Hach, L. J. Tippett, and D. R. Addis, "The Simpson's paradox and fMRI: Similarities and differences between functional connectivity measures derived from within-subject and across-subject correlations," *Neuroimage*, vol. 135, pp. 1–15, Jul. 2016, doi: 10.1016/J.NEUROIMAGE.2016.04.028.

[99] Y. Benjamini and Y. Hochberg, "Controlling the False Discovery Rate: A Practical and Powerful Approach to Multiple Testing," *Journal of the Royal Statistical Society: Series B (Methodological)*, vol. 57, no. 1, pp. 289–300, Jan. 1995, doi: 10.1111/J.2517-6161.1995.TB02031.X.

Appendix

ROI	Left						Right					
	Contrast	Estimate	SE	df	t.ratio	p.value	Contrast	Estimate	SE	Df	t.ratio	p.value
FEF	hMT - Parietal	-0.2713	0.416	401	-0.652	0.8696	hMT - Parietal	-0.4496	0.416	401	-1.081	0.4208
	hMT - Sham	-0.0358	0.416	401	-0.086	0.9316	hMT - Sham	0.1608	0.416	401	0.386	0.6994
	Parietal vs Sham	0.2356	0.425	401	0.554	0.8696	Parietal vs Sham	0.6104	0.425	401	1.436	0.4208
hMT	hMT - Parietal	-0.6628	0.416	401	-1.593	0.1119	hMT - Parietal	-0.1174	0.416	401	-0.282	0.7780
	hMT - Sham	0.7152	0.416	401	1.719	0.1119	hMT - Sham	0.5865	0.416	401	1.410	0.2392
	Parietal vs Sham	1.3780	0.425	401	3.242	0.0039	Parietal vs Sham	0.7038	0.425	401	1.656	0.2392
IFJ	hMT - Parietal	-0.4338	0.416	401	-1.043	0.7344	hMT - Parietal	-0.4135	0.416	401	-0.994	0.4814
	hMT - Sham	-0.1399	0.416	401	-0.336	0.7369	hMT - Sham	0.0366	0.416	401	0.088	0.9300
	Parietal vs Sham	0.2939	0.425	401	0.692	0.7344	Parietal vs Sham	0.4501	0.425	401	1.059	0.4814
IPS	hMT - Parietal	-0.7819	0.416	401	-1.879	0.1828	hMT - Parietal	0.0353	0.416	401	0.085	0.9323
	hMT - Sham	-0.2211	0.416	401	-0.531	0.5954	hMT - Sham	0.8859	0.416	401	2.129	0.0691
	Parietal vs Sham	0.5608	0.425	401	1.320	0.2816	Parietal vs Sham	0.8505	0.425	401	2.001	0.0691
Ant IPS	hMT - Parietal	-1.0075	0.416	401	-2.422	0.0238	hMT - Parietal	-0.3062	0.416	401	-0.736	0.4621
	hMT - Sham	0.0541	0.416	401	0.130	0.8965	hMT - Sham	0.8762	0.416	401	2.106	0.0537
	Parietal - Sham	1.0617	0.425	401	2.498	0.0238	Parietal vs Sham	1.1824	0.425	401	2.782	0.0170
Post IPS	hMT - Parietal	-0.4238	0.416	401	-1.019	0.3090	hMT - Parietal	-0.7931	0.416	401	-1.906	0.0860
	hMT - Sham	1.0413	0.416	401	2.503	0.0191	hMT - Sham	0.4753	0.416	401	1.142	0.2540
	Parietal vs Sham	1.4651	0.425	401	3.447	0.0019	Parietal vs Sham	1.2684	0.425	401	2.984	0.0090
TPJ	hMT - Parietal	-0.4360	0.416	401	-1.048	0.5564	hMT - Parietal	-0.4704	0.416	401	-1.131	0.4484
	hMT - Sham	-0.0553	0.416	401	-0.133	0.8943	hMT - Sham	-0.0284	0.416	401	-0.068	0.9457
	Parietal vs Sham	0.3807	0.425	401	0.896	0.5564	Parietal vs Sham	0.4420	0.425	401	1.040	0.4484
Ant TPJ	hMT - Parietal	-	-	-	-	-	hMT - Parietal	0.1454	0.416	401	0.350	0.7906
	hMT - Sham	-	-	-	-	-	hMT - Sham	0.2584	0.416	401	0.621	0.7906
	Parietal vs Sham	-	-	-	-	-	Parietal vs Sham	0.1129	0.425	401	0.266	0.7906
Post TPJ	hMT - Parietal	-0.0971	0.416	401	-0.233	0.9508	hMT - Parietal	-0.6807	0.416	401	-1.636	0.1539
	hMT - Sham	-0.1233	0.416	401	-0.296	0.9508	hMT - Sham	0.0427	0.416	401	0.103	0.9184
	Parietal vs Sham	-0.0262	0.425	401	-0.062	0.9508	Parietal vs Sham	0.7234	0.425	401	1.702	0.1539
VFC	hMT - Parietal	-0.5409	0.416	401	-1.300	0.2914	hMT - Parietal	-0.6973	0.416	401	-1.676	0.2354
	hMT - Sham	0.0478	0.416	401	0.115	0.9085	hMT - Sham	-0.0946	0.416	401	-0.227	0.8202
	Parietal vs Sham	0.5888	0.425	401	1.385	0.2914	Parietal vs Sham	0.6027	0.425	401	1.418	0.2354

Table 1 Appendix. Results of the contrasts between Stimulation conditions for each ROI divided per hemisphere embedded in the DVAN relative to the OD task. For each level of brain area (ROI), *statistical details are reported comprising estimated marginal means for each combination of Stimulation factor, along with SE, t ratio and corresponding p value (FDR-corrected).*

ROI	ChiSq	Df	Pr(>Chisq)
FEF	3.0279	2	0.2200
hMT	8.2966	2	0.0158
IFJ	3.7083	2	0.1566
IPS	1.4832	2	0.4764
Ant IPS	1.0495	2	0.5917
Post IPS	1.3139	2	0.5184
TPJ	3.8990	2	0.1423
Post TPJ	0.5534	2	0.7583
VFC	2.5490	2	0.2796

Table 2 Appendix. Results of the LMM for each ROI embedded in the DVAN, with data collapsed across hemispheres for the TOJ task. For each brain area (left and right hemisphere data were collapsed), *statistical details of the LMM fitted (lmer(normalized_delta ~ Condition + (1|subj), data=df_ROI) are reported comprising of Chi-square and corresponding p-value of the model.*

ROI	Left						Right					
	Contrast	Estimate	SE	df	t.ratio	p.value	Contrast	Estimate	SE	Df	t.ratio	p.value
FEF	hMT - Parietal	-0.2639	0.427	386	-0.618	0.8359	hMT - Parietal	-0.2735	0.427	386	-0.641	0.9070
	hMT - Sham	-0.0885	0.427	386	-0.207	0.8359	hMT - Sham	-0.0499	0.427	386	-0.117	0.9070
	Parietal vs Sham	0.1754	0.436	386	0.402	0.8359	Parietal vs Sham	0.2235	0.436	386	0.513	0.9070
hMT	hMT - Parietal	-0.3496	0.427	386	-0.819	0.6200	hMT - Parietal	-0.5596	0.427	386	-1.311	0.5721
	hMT - Sham	0.1611	0.427	386	0.377	0.7061	hMT - Sham	-0.3565	0.427	386	-0.835	0.6063
	Parietal vs Sham	0.5107	0.436	386	1.171	0.6200	Parietal vs Sham	0.2031	0.436	386	0.466	0.6416
IFJ	hMT - Parietal	-0.5596	0.427	386	-1.311	0.5721	hMT - Parietal	-0.4761	0.427	386	-1.115	0.6306
	hMT - Sham	-0.3565	0.427	386	-0.835	0.6063	hMT - Sham	-0.2662	0.427	386	-0.623	0.6306
	Parietal vs Sham	0.2031	0.436	386	0.466	0.6416	Parietal vs Sham	0.2099	0.436	386	0.481	0.6306
IPS	hMT - Parietal	-0.6729	0.427	386	-1.576	0.1737	hMT - Parietal	-0.0767	0.427	386	-0.180	0.8575
	hMT - Sham	-0.9645	0.427	386	-2.259	0.0733	hMT - Sham	0.3448	0.427	386	0.808	0.6298
	Parietal vs Sham	-0.2916	0.436	386	-0.669	0.5041	Parietal vs Sham	0.4215	0.436	386	0.966	0.6298
Ant IPS	hMT - Parietal	-0.8303	0.427	386	-1.945	0.1575	hMT - Parietal	0.3653	0.427	386	0.856	0.5891
	hMT - Sham	-0.1777	0.427	386	-0.416	0.6775	hMT - Sham	0.3915	0.427	386	0.917	0.5891
	Parietal vs Sham	0.6526	0.436	386	1.497	0.2030	Parietal vs Sham	0.0263	0.436	386	0.060	0.9520
Post IPS	hMT - Parietal	-0.2552	0.427	386	-0.598	0.5503	hMT - Parietal	-0.0426	0.427	386	-0.100	0.9205
	hMT - Sham	0.3007	0.427	386	0.704	0.5503	hMT - Sham	0.2478	0.427	386	0.581	0.8428
	Parietal vs Sham	0.5560	0.436	386	1.275	0.5503	Parietal vs Sham	0.2905	0.436	386	0.666	0.8428
TPJ	hMT - Parietal	-0.1764	0.427	386	-0.413	0.6796	hMT - Parietal	-0.0697	0.427	386	-0.163	0.8704
	hMT - Sham	-0.3965	0.427	386	-0.929	0.6796	hMT - Sham	-0.6026	0.427	386	-1.411	0.3337
	Parietal vs Sham	-0.2200	0.436	386	-0.505	0.6796	Parietal vs Sham	-0.5329	0.436	386	-1.222	0.3337
Ant TPJ	hMT - Parietal	-	-	-	-	-	hMT - Parietal	0.3594	0.427	386	0.842	0.6005
	hMT - Sham	-	-	-	-	-	hMT - Sham	-0.0351	0.427	386	-0.082	0.9345
	Parietal vs Sham	-	-	-	-	-	Parietal vs Sham	-0.3946	0.436	386	-0.905	0.6005
Post TPJ	hMT - Parietal	0.0472	0.427	386	0.111	0.9120	hMT - Parietal	-0.1401	0.427	386	-0.328	0.7430
	hMT - Sham	-0.1639	0.427	386	-0.384	0.9120	hMT - Sham	-0.3066	0.427	386	-0.718	0.7430
	Parietal vs Sham	-0.2111	0.436	386	-0.484	0.9120	Parietal vs Sham	-0.1665	0.436	386	-0.382	0.7430
VFC	hMT - Parietal	-0.4765	0.427	386	-1.116	0.5917	hMT - Parietal	-0.5900	0.427	386	-1.382	0.5034
	hMT - Sham	-0.2424	0.427	386	-0.568	0.5917	hMT - Sham	-0.4092	0.427	386	-0.959	0.5075
	Parietal vs Sham	0.2341	0.436	386	0.537	0.5917	Parietal vs Sham	0.1807	0.436	386	0.414	0.6788

Table 3 Appendix. Results of the contrasts between Stimulation conditions for each ROI divided per hemisphere embedded in the DVAN relative to the TOJ task. For each level of brain area (ROI), *statistical details are reported comprising estimated marginal means for each combination of Stimulation factor, along*